8   Development of actinide speciation methods

Maintaining a state-of-the-art portfolio of advanced surface science and spectroscopy methods at INE is an important R&D activity, as these methods are crucial tools for advancing our understanding of actinide and radionuclide (geo)chemistry or the behavior of nuclear waste forms during prolonged interim storage. Radionuclide speciation methods available at INE radiochemical laboratories and the KIT synchrotron radiation facility ANKA are continuously adapted to serve the requirements of the INE in house R&D program. Access to this unique instrumentation is as well provided to INE's national and international partners in the frame of cooperation agreements or joint research projects. As a major milestone in instrumentation development, in 2016 the new CAT-ACT hard X-ray beamline for CAT*alysis* and ACT*inide* research at ANKA became fully operational. The new ACT lab for synchrotron based radionuclide speciation studies - operated by INE in addition to the existing INE-Beamline - was fully equipped and licensed to handle radioisotopes with activities up to one million times the European exemption limit. The multi analyzer-crystal (MAC) X-ray emission spectrometer previously commissioned at the INE-Beamline was moved to the ACT station, where it has already shown to provide unprecedented insight into electronic and bonding characteristics of radionuclides in highly active nuclear materials, e.g., with the characterization of Pu oxidation states in borosilicate glasses by high resolution Pu M_5-edge XANES spectroscopy. The portfolio of laser based speciation techniques at INE comprises different optical and non-optical methods: LIBD, TRLFS, LIBS, and LA-ICP-MS (the latter in collaboration with JRC-ITU). Currently, an ambitious program to upgrade all existing systems and to improve their performance is under way. In this context, a new mobile setup for TRLFS-based U(VI) speciation studies was built and successfully commissioned in 2016. Processes determining radionuclide retention or release from nuclear waste matrices are generally controlled by surface reactions. Applying angle-dependent photoelectron spectroscopy (ADXPS), formation of an U_4O_9 (U(IV,V)) surface oxide underneath a thin (~0.5 nm) hydroxylated layer was observed on a sintered and annealed UO_2 pellet exposed for 15 months to ambient conditions. Nuclear magnetic resonance spectroscopy (NMR) gives direct insight into metal-ligand bonding phenomena relevant for complex formation and selectivity studies in the field of actinide / lanthanide separation chemistry. In 2016, a combined NMR and Cm-TRLFS investigation allowed to explain the unexpected extraction kinetics of a new bis-pyrazolyl pyridine (C4-BPP) ligand observed in initial actinide extraction studies. A method more recently established at INE is accelerator mass spectrometry (AMS). AMS is presently one of the most sensitive analytical techniques with an overall sensitivity of ~10^4 atoms in a sample. The analytical capability to determine concentrations of actinides and long lived fission products (like ^{99}Tc) in natural samples at ultra-trace levels (fg/g and ag/g) is of great relevance both for environmental studies and for in situ tracer tests or diffusion experiments as, e.g., in the frame of the CFM project at the Grimsel test site. Many of the in-house research activities at INE benefit from strong support by quantum chemical calculations, providing molecular structures or thermodynamic data. The systems under investigation vary from small complexes in solution to crystals or interfaces. New algorithms and the constantly improving hardware allow to get continuously closer to a detailed description of radionuclide systems at the level of electronic structures, thus directly complementing experimental results.

8.1   R&D projects conducted at the INE-Beamline for actinide research and the new CAT-ACT beamline at ANKA

S. Bahl, A. Bauer, E. Bohnert, K. Dardenne, E. González-Robles, M. Herm, V. Krepper, V. Metz, I. Pidchenko, J. Rothe, M. Vespa, T. Vitova

In co-operation with:

J.-D. Grunwaldt[a], H. Lichtenberg[a], T. Prüßmann[b], A. Zimina[b], T. Spangenberg[c], R. Steininger[c], S. Mangold[c], S. Peuget[d], J. Delrieu[d], C. Jégou[d]

Karlsruhe Institute of Technology, [a]Institute for Chemical Technology and Polymer Chemistry (ITCP), [b]Institute for Catalysis Research and Technology (IKFT); Karlsruhe Institute of Technology, [c]Institute for Photon Science and Synchrotron Radiation (IPS); [d]Institut de Chimie Séparative de Marcoule, CEA Valrhô Marcoule, UMR 5257, BP 17171, 30207 Bagnols-sur-Cèze, France

Introduction

Synchrotron radiation (SR) based speciation techniques have become key methods in basic and applied radionuclide research. This development is primarily driven by the need to secure molecular-scale understanding for (geo-)chemical processes determining the mobility of long-lived radionuclides possibly released from a projected disposal site for highly active, heat producing nuclear waste (HAW). Presently, final disposal in deep bedrock repositories is deemed as the preferred option for the management of spent nuclear fuel (SNF) and high level waste (HLW) glass used for conditioning of highly radioactive residues from nuclear fuel reprocessing. Solving the nuclear disposal safety case requires the assessment of an envisaged

disposal site on geological time scales, where speciation techniques like XAS (X-ray Absorption Spectroscopy) and XES (X-ray Emission Spectroscopy) provide necessary input parameters to model the geochemical behavior of radionuclides. More recently, as well attempts to directly characterize HAW matrices by XAFS techniques came into focus, mainly due to the necessity to assess effects of an extended interim storage period preceding deep geological disposal, e.g., embrittlement of fuel pin claddings.

The INE-Beamline for radionuclide science [1] at the KIT synchrotron source ANKA became fully operational in 2005 as a flexible experimental station for X-ray based radionuclide speciation investigations. One decade later, the commissioning of the new hard X-ray beamline 'CAT-ACT' for CATalysis and ACTinide research at ANKA has been completed [2] and the ACT lab for synchrotron based radionuclide speciation studies fully equipped and licensed to handle radioisotopes with activities up to one million times the exemption limit. The multi analyzer-crystal (MAC) X-ray emission spectrometer previously commissioned at INE-Beamline will serve as core component of the experimental infrastructure at the ACT lab. The INE-Beamline and the ACT experimental station are the only facilities of their kind in Europe offering direct access to radiochemistry laboratories operating a shielded box-line in close proximity to the synchrotron light source on the same research campus.

INE-Beamline user operation in 2016

After conversion of ANKA from a LK-II national user facility to a LK-I KIT internal research infrastructure in 2015, beamline operation had to be rearranged in 2016 to suit new boundary conditions, first of all a markedly reduced availability of beamtime shifts. Future ANKA operation under the auspices of the newly founded KIT Institute for Accelerator Physics and Technology (IBPT) foresees a combined use of the ANKA storage ring as SR source and testbed for the development of accelerator technology - including insertion devices, electron beam sources and beam diagnostic tools. As a consequence of ANKA restructuring beamtime distribution is no longer based on a peer review proposal process, but on in house needs within the KIT and HGF research programs and individual agreements between beamline operators and external cooperation partners.

For 2016, a total of 73 days of standard SR operation days had been initially projected (compared to 126 days in 2014) – 19 days (about 25%) of those were lost due to storage ring and beam quality failure. The remaining days were spent for INE in-house research (35%), beamline development and maintenance (10%) and external beamtime projects (30%). Nevertheless, still a total of 20 in house and external projects were successfully carried out at the beamline. For the first time, in 2016 limited user operation was also offered at the new ACT endstation after completion of the experimental setup (cf. the following section). As in previous years, INE in house projects in

2016 covered the investigation of a broad range of materials containing actinides (*An*), fission products or their chemical homologues in the context of nuclear waste disposal safety research or basic actinide chemistry. These studies comprised the investigation of Np(V) complexation by chloride, µ-focus investigations of irradiated SNF cladding fragments (described in more detail below), the effect of chemical pressure on the local structure of Eu^{3+} in $M(OH)_3$ (M = La, Y), in-situ XRD and XAFS investigations of Pu(III/IV)-ISA complexation, the redox behavior of U(VI/IV) in acidic to hyper-alkaline conditions, the solubility of U(IV) under reducing conditions in the absence and presence of carbonate or XANES measurements to identify the redox-state and speciation of As in geothermal scaling samples containing radioactive Pb-210. Several further projects received beamtime as pilot experiments during commissioning of the XAFS detection systems in the ACT laboratory, e.g., a XAS study of the co-adsorption of Se(IV) and Sr(II) on goethite. Some of these studies are presented in more detail elsewhere in this annual report. A study focusing on the advanced high resolution X-ray emission techniques (HRXES) in the tender X-ray regime (actinide M-edges) - now possible at the ACT station – is highlighted in the last section below.

HGF external scientists from the German and international research institutions listed below conducted research at the INE-Beamline in 2016:

- FZ Jülich / IEK-6, Germany
- Heidelberg University, Germany
- CEA Cadarache, France
- JRC Karlsruhe, European Commission

As in the preceding years a considerable share of INE in house beamtime was spent for experiments conducted by master and graduate students in the frame of their thesis projects.

Commissioning of the ACT experimental station and upgrades at the INE-Beamline

To secure reliable beamline operation for in house and cooperation partner requirements and to exploit
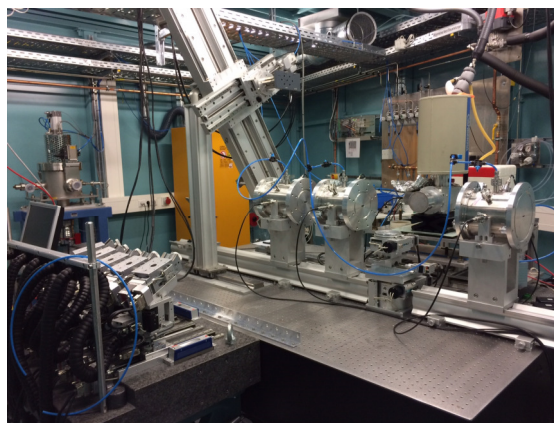
Fig. 1: *XAFS and XES detection setup at the ACT experimental station.*

limited ANKA SR operation at utmost efficiency, maintenance and consequent infrastructure upgrading are mandatory at both beamline facilities in INE's responsibility. The year 2016 was characterized by the challenge to replace major components at INE-Beamline and to setup an entirely new XAFS data acquisition system at the ACT experimental station – including capabilities for high resolution X-ray emission spectroscopy (HRXES), standard X-ray transmission and X-ray fluorescence (XRF) detection. Exchangeability of components and control software macros was intended to keep maintenance efforts at a reasonable level.

After installation of the 2.1×1.4 m^2 optical table (Newport, France), the main components of the Johann-type MAC spectrometer (analyzer crystal and detector stages) were craned into the ACT hutch and precisely aligned to a permanent position relative to the X-ray focus inside the hutch defined by the toroidal second mirror of the CAT-ACT optic. The crystal and detector positioning system was extended by a 4 axis (x,y,z,φ) sample positioning stage (Huber Diffraktionstechnik, Germany). For standard XAFS data acquisition, an optical bench based on X-95 profile rails holding three ionization chambers for parallel absorption and reference sample measurements (Poikat, Germany) was installed. The 5-pixel LEGe solid state fluorescence detector (Canberra, Belgium) – previously operated at INE-Beamline – was finally moved to ACT, as it permits detection of high energy photons up to the Kα lines of the early lanthanides accessible at the new beamline. The whole setup is depicted in Fig. 1.

Although CAT-ACT with its 2.5 T superconducting wiggler source is optimized for hard X-ray operation, the achievable low spectral limit of ~3.4 keV in the tender X-ray regime permits highly efficient absorption and emission spectroscopy at the *An* M edges (the U M4-edge, e.g., is at 3.73 keV). To avoid scattering and absorption in air, at these energies all beam paths can be kept in He atmosphere by installation of a temporary gas tight structure consisting of a rigid plexiglass frame bolted to the experiment table, which spans two flexible bags surrounding the analyzer crystals and the detector which are movable along vertical Rowland circles. Commissioning of the ACT station was completed after final tests of the ventilation system, providing about -20 Pa lower pressure inside the experiment hutch which can be designated as a temporary controlled area. A license for handling doubly contained samples with radionuclide activities up to one million times the exemption limit (with the exception of 200 mg each for the fissile isotopes U-235 and Pu-239 and 10^5 times the exemption limit for Pa-231) is provided, following the same safety concept previously implemented at the INE-Beamline.

The LEGe detector dismounted at the INE-Beamline was replaced by a thermoelectrically cooled 4-pixel Vortex ME4-multichannel system (Hitachi High-Technologies Science America, USA), which can be read-out in parallel with the existing Vortex-60VX

manufactured by the same company. At both experimental stations, state-of-the-art digital X-ray pulse processors (XIA xMap DXP, USA) have been commissioned and integrated into the SPEC-based data acquisition system. Furthermore, at INE-Beamline the ageing DCM Bragg-axis servo motor controller was replaced by a state-of-the-art system (Newport XPS, France), which allows for angle encoder controlled closed loop positioning with a resolution of 1E-4 degree/step.

XAS, µ-XAS and µ-XRF investigation of an irradiated SNF cladding ring segment

In the light of a yet unclear timeframe for the necessary site selection, construction and licensing procedure before a final HAW repository becomes operational in Germany, a significant prolongation of SNF interim storage above surface (> 40 a) has to be considered. In this context, the possibly limited integrity of fuel pins - affecting SNF transportability and conditioning prior to final disposal - is of major concern. Hence, a better understanding of the effects of thermal, mechanical and radiological stress on fuel pin claddings is mandatory. Research at INE focuses on Zircaloy-4 – a cladding material commonly used in PWR fuel rod assemblies – both with respect to the formation of activation nuclides (cf. chapter 5.1) during reactor operation and the possible hull material corrosion induced by blueish-black deposits of volatile fission products observed on the inner cladding surface. In 2016 Zircaloy-4 cladding ring segments
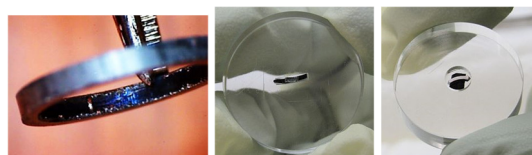

Fig. 2: *Zircaloy-4 cladding ring cut from fuel rod plenum section (left) with blueish deposit on inner surface; ring fragments mounted to expose inner surface (middle) and cross-section (right hand side image).*
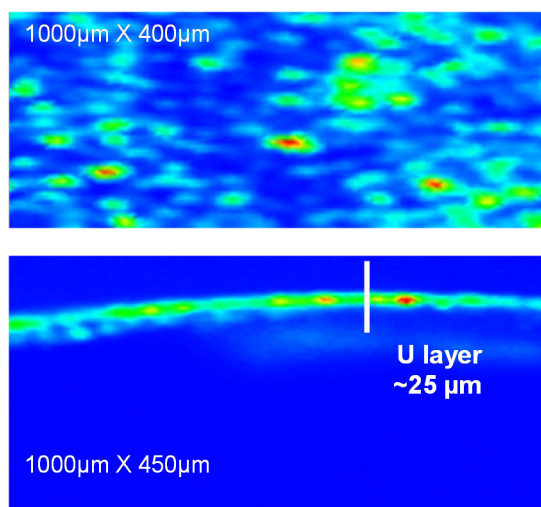
Fig. 3: *U Lα fluorescence images of (top) the inner cladding surface and (bottom) the ring cross section.*

Sample	Melting temperature (°C)	m(PuO_2) (wt%)	Atmosphere	Crucible material	R
G1	1200	0.85	Ar	Pt	0
G2	1400	2.0	Ar	Pt	0.37
G3	1400	4.0	Ar	Pt	0.56
G4	1400	8.0	Ar	Pt	0.73
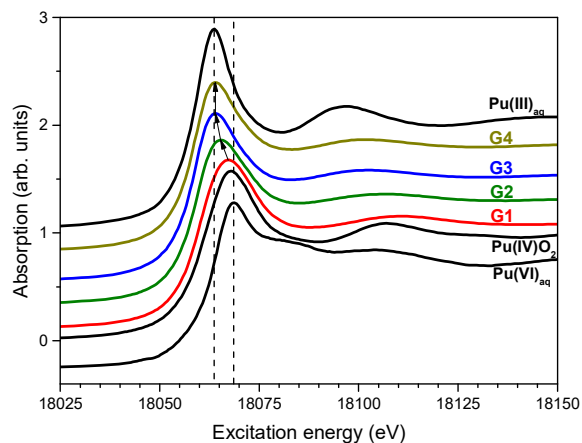
Fig. 4: *Pu L_3 edge XANES spectra of the G1-G4 glasses and the Pu(III)$_{aq}$, Pu(IV)O$_2$, Pu(VI)$_{aq}$ references.*

for investigation by SR-based methods were sampled from the plenum section of a fuel rod irradiated in the Swiss PWR Gösgen (average burn-up: 50.4 GWd/tHM). These measurements represent to our knowledge the first attempts ever made to characterize cladding materials from irradiated fuel with XAS and XRF techniques at a SR beamline facility. Two mm-sized cladding fragments cut from a hull material ring (contact dose rate ~30 µSv/h) were sealed in acryl glass sample holders allowing for exposure of the inner surface or the cross section towards the incident beam (cf. Fig. 2) and transferred to the INE-Beamline. U L3 bulk XAS and µ-XAS measurements for elements identified in µ-XRF distribution maps with a lateral resolution of better than 20 µm were performed for both samples in fluorescence detection mode. Excitation energies were kept below the Zr K-edge (17.998 keV) to avoid saturation of the Vortex fluorescence detector.

Surprisingly, uranium was detected as most abundant element (besides Zr which was not excited) omnipresent on the inner cladding surface – mostly concentrated in hot spots of a few tens of µm diameter (Fig. 3, top). As this part of the fuel hull was not in contact with UO_2 pellets during fuel burnup in the reactor, it has to be assumed that most of the uranium was originally deposited by abrasion during manufacturing of the fuel rods. The µ-XRF scan of the cladding ring segment cross section in Fig. 3 (bottom) exposes a marked uranium layer of about 25 µm thickness following the curvature of the inner surface (note that the blue zero-intensity area below this curve

depicted in Fig. 3 represents the acryl glass backside of the sample containment, while the blue zone above corresponds to the zirconium alloy). µ-focus U L3 XANES spectra obtained from the cross-section layer and bulk U L3 XANES spectra obtained from the inner surface (beam dimension ~600 µm × 300 µm) exhibit the typical $U^{IV}O_2$ fluorite-type signature, yet with a significantly increased white line intensity – likely a particle size effect pointing to the presence of small UO_2 entities at the inner cladding surface. Preliminary U L3 EXAFS analysis does not provide clear evidence for U-Zr backscattering, thus U does not seem to be incorporated in the Zircaloy-4 matrix, but rather dispersed as oxide nanoparticles in groves or small cracks. Besides uranium, a multitude of elements was detectable on the inner cladding surface, some of them probably deposited as volatile fission products (e.g., Hg, Rb, Ba, Ti), while some (Fe, Cu, Ni) were detected as metallic particles, probably originating from sawing and sample conditioning. Unambiguous detection of cesium and iodine, both by excitation at their L3 absorption edges at 5.012 keV and 4.557 keV, respectively, was not possible due to reabsorption of their soft fluorescence photons in the UO_2 matrix or the sample containment. Future attempts will focus on the detection of these elements which are of special relevance as possibly mobile and bioavailable fission nuclides by hard X-ray K-edge measurements (Cs(0) 1s: 35.985 keV, I(0) 1s: 33.169 keV) at the ACT station.

Comparison of Pu L3-XANES with M5 HR-XANES for characterization of Pu oxidation states in borosilicate glasses

Tailored glass compositions and vitrification processes leading to desired oxidation states of the *An* elements require sensitive characterization methods. One of the widely-used tools for determination of the oxidation states of the *An* elements is the *An* L_3 edge XANES technique. However, due to the large core-hole lifetime broadening contributing to the *An* L_3 edge XANES (e.g., Pu $2p_{3/2}$: 7.8 eV), the spectrum is insensitive to the presence of minor amounts of *An* oxidation states. Deschanels *et al*. studied the Pu solubility in borosilicate glass and prepared several homogeneous glasses with increasing Pu content (0.85 - 8 wt% PuO_2) and variable amount of reducing agent (cf. Table 1). [3] They characterized the Pu oxidation state by the Pu L_3 edge XANES technique and reported stabilization of Pu in its tetra- and trivalent oxidation states. We have reexamined the oxidation states of Pu in the same glass samples applying the more advanced Pu M_5 edge high energy resolution XANES (HR-XANES) method. The *An* $M_{4,5}$ HR-XANES technique recently emerged as a valuable direct probe of the *An* 5f valence orbitals, which are largely responsible for the chemical bonding in the *An* compounds [4]. It was demonstrated that the spectra are very sensitive to the *An* oxidation states and allow, e.g., to distinguish between U(IV), U(V) and U(VI) species when mixed in the same material - not easily

possible with other spectroscopy techniques [5]. This method probes the bulk of the material (1 µm penetration depth) and does not require vacuum conditions as, e.g., the laboratory based surface sensitive X-ray photoelectron spectroscopy (1 - 10 nm penetration depth). Due to the drastically reduced core-hole lifetime broadening (0.5 eV) contributing to the spectrum compared to the Pu L_3 absorption edge (7.8 eV) and the improved experimental energy resolution, the spectral resolution is significantly enhanced, providing more reliable access to the *An* oxidation states.

Here we provide new insight into the redox behavior of Pu, which controls its solubility in glass matrices. The Pu oxidation states are correlated to the applied vitrification conditions and the added amount of reducing agent. The first application of the Pu M_5 edge HR-XANES technique for oxidation state characterization of Pu with the specific example of Pu incorporated into borosilicate glasses is reported. We demonstrate the need for development and application of such advanced methods for investigations of complex nuclear waste matrices.

The Pu doped borosilicate glasses were synthesized in the Atalante laboratories of the Commissariat à l'énergie atomique et aux énergies alternatives (CEA) Marcoule Centre, France. The chemical compositions of the Pu doped borosilicate glasses and the preliminary structural analyses can be found in the publication by Deschanels et al. [3]. The investigations discussed below are performed within the frame of the TALISMAN project TALI-C03-01 in collaboration with Sylvain Peuget, CEA Marcoule Centre.

Pu L_3 edge XANES: Fig. 4 depicts the Pu L_3 edge XANES spectra of the Pu doped G1-G4 glass samples and the Pu(III)$_{aq}$, Pu(IV)O$_2$, Pu(VI)$_{aq}$ reference materials. The experiments were performed at the INE-Beamline. The Pu L_3 edge XANES spectra mainly describe dipole allowed electronic transitions from 2p to unoccupied 6d orbitals (2p$_{3/2}$ → 6d). The energy positions of the abrupt increase in absorption (absorption edge) and the most intense absorption resonance (white line, WL) typically shift to higher energies by reduction of the electronic density in the vicinity of the Pu atom nucleus; this energy shift of the spectrum is commonly used for oxidation state analysis. However, the spectra can also shift due to changes in the short and long-range atomic environment around the absorbing atom. A well-known challenge is to differentiate between Pu(IV) and Pu(VI), where the latter tends to form short trans-dioxo bonds with lengths of 1.75 Å (Pu-yl, plutonyl) in both solid and liquid states. Due to the strong covalence of the plutonyl bond, there is an accumulation of electronic charge on the Pu atoms. As a result, the 2p core-hole is well screened and the WL positions of the Pu(VI) and the Pu(IV) spectra can coincide (cf. Fig. 4). Note that the Pu L_3 edge XANES of Pu(V) trans-dioxo species (axial bond length around 1.94 Å) is even shifted to lower energies compared to the spectrum of Pu(IV).

A trend indicated with solid black arrows can be observed in the spectra. The energy position of the WL of the G1 spectrum is slightly shifted to lower ener-

gies compared to the WL of the Pu(IV) reference spectrum, suggesting contribution of Pu(III) in the G1 sample. For R values < 0.73 (G1-G3), mixtures of most likely tri- and tetravalent Pu are formed. The energy positions of the WLs of the G4 (R = 0.73) and the Pu(III) spectra coincide, affirming the efficient reduction of Pu(IV) to Pu(III) in the G4 glass caused by the reducing agent Si$_3$N$_4$.

These results are in good agreement with the report of Deschanels *et al.*, who also applied the Pu L_3 edge XANES technique to investigate the Pu oxidation states in the glasses G1-G3. [3] However, these analyses cannot exclude potential stabilization of minor amounts of higher Pu oxidation states.

Pu M_5 edge HR-XANES: Fig. 5 depicts the Pu M_5 edge HR-XANES spectra of the G1-G4 glass samples and the Pu(III)$_{aq}$, Pu(IV)O$_2$, Pu(VI)$_{aq}$ reference materials. These experiments were performed at the INE-Beamline, whereas the spectra depicted in Fig. 6 were recorded at the new ACT experimental station. The
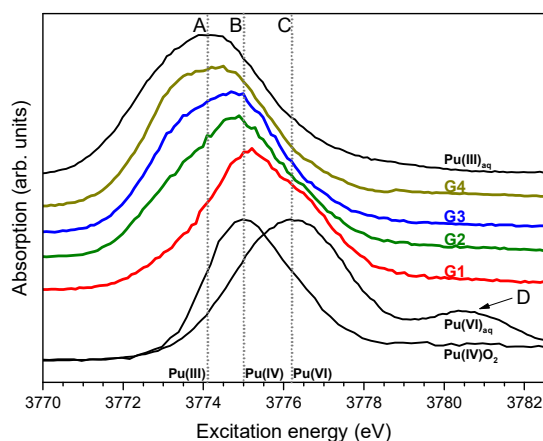
Fig. 5: *Pu M_5 edge HR-XANES spectra of the G1-G4 glasses, Pu(IV)O$_2$ reference and the Pu(III)$_{aq}$, Pu(VI)$_{aq}$ references recorded with medium and low experimental energy resolution, respectively.*
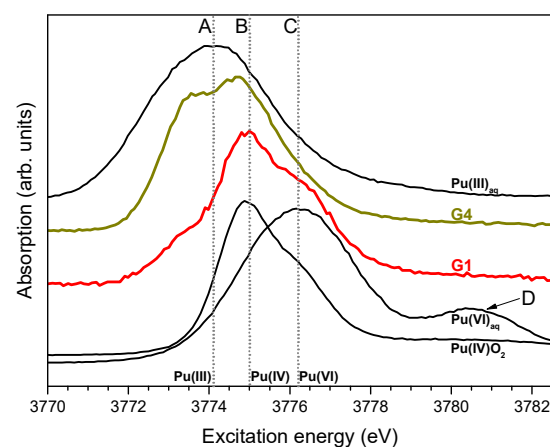
Fig. 6: *Pu M_5 edge HR-XANES spectra of the G1, G4 glasses, Pu(IV)O$_2$ reference and the Pu(III)$_{aq}$, Pu(VI)$_{aq}$ references recorded with high and low experimental energy resolution, respectively.*

MAC spectrometer described above was used for both experiments. Due to the higher photon flux at the CAT-ACT beamline, it was possible to achieve higher experimental resolution, the beam size was confined to 500×500 μm^2 size by applying a pinhole in front of the sample and additional masks giving access only to the central section of the five Si(220) analyzer crystals.

The Pu M_5 edge HR-XANES spectra describe the dipole allowed transitions of 3d electrons to 5f unoccupied orbitals (3d$_{3/2}$ → 5f), which contain most of the *An* valence electrons participating in the chemical bonding. The valence electronic configuration of metallic Pu is 7s^{2}5f^6. In contrast to the Pu L_3 edge XANES spectra, the Pu M_5 edge HR-XANES reference spectra clearly shift to higher energies in the order Pu(III), Pu(IV), Pu(VI); Pu(V) is difficult to stabilize, therefore no reference spectrum is presented. The spectra of the Pu(III)$_{aq}$ and Pu(VI)$_{aq}$ references were recorded with lower experimental energy resolution. This results in a larger broadening of the spectra. Considering the PuO$_2$ spectra measured with variable experimental energy resolutions a shift towards lower energies of up to 0.1 eV can be expected for Pu(III)$_{aq}$ and Pu(VI)$_{aq}$ spectra if measured with a resolution comparable to the glass spectra.

The G1 and the Pu(IV) spectra have very similar energy positions (cf. Fig. 5, line B), which is a strong indication that Pu(IV) is the main species in the G1 sample. The G2-G4 spectra are shifted to lower energies with increasing R; the spectrum of G4 peaks at about the energy position of line A (3774.1 eV) marking the most intense absorption resonance of the Pu(III) reference spectrum. This general trend suggests a reduction of the Pu oxidation state going from G1 to G4 in agreement with the Pu L_3 edge results. However, the G1-G4 spectra have asymmetric shapes. There are shoulders on the low (3774.1 eV) and high energy (3776.5 eV) sides of the G1 spectrum, which increase and decrease in intensity, respectively, going from the G1 to the G4 spectrum. These additional spectral features point to mixtures of Pu(III) (line A), Pu(IV) (line B) and a higher oxidation state of Pu. We infer that this spectral contribution is likely due to the presence of Pu(VI) (line C). Note that the shoulder positioned next to line C on the high-energy side of the main peaks of the G1 and G2 spectra (3776.5 eV) nearly coincides with the main peak of the Pu(VI) reference. Pu(V) is less probable but it might be potentially stabilized in the glass matrix as well, therefore we cannot completely exclude its presence.

The G1, G4 and PuO$_2$ spectra recorded with even higher experimental energy resolution are depicted in Fig. 6. The shoulder C is well pronounced in the G1 spectrum, affirming the formation of Pu species with higher than +IV oxidation state. The low energy shoulder corresponding to minor contribution of Pu(III) is now clearly distinguishable in the G1 spectrum. The high-energy resolution enables also distinct detection of Pu(III) and Pu(IV) in the G4 glass. The spectrum demonstrates formation of similar amounts of Pu(III) and Pu(IV).

The post-edge feature D in the Pu(VI) reference spectrum is characteristic for plutonyl [4,6] and describes transitions to the sigma antibonding (σ^*) molecular orbital. [6]. A similar peak was reported recently also for uranyl by Vitova *et al*. [4]. As feature D is not present in the spectra of G1 and G2, we conclude that the potential Pu(VI) species does not form a plutonyl type of bonding. It is more likely that the Pu-O distances are elongated and Pu is coordinated by a more symmetric set of O atoms than in the plutonyl case, i.e., in a plutonate structure.

In summary, the Pu M5 edge HR-XANES method is clearly capable of detecting Pu(III), Pu(IV) and Pu(VI) being simultaneously present in a nuclear glass sample. Quantitative analyses of the Pu species with different oxidization states are possible when spectra of appropriate reference materials are recorded under the same experimental conditions. Our study demonstrates that this characterization method can be used for monitoring the redox conditions in vitrification processes upon reductant addition. A clear correlation of Pu oxidation state distribution and added amount of the reductant is revealed. For complete reduction of Pu to the trivalent state in glass with similar chemical composition it would be necessary to adjust R to a value higher than 0.73. This will most likely further increase the Pu loading in the glass.

We also clearly detected for the first time the formation of Pu(VI) species in glasses synthesized upon addition of a Pu nitric acid solution to the glass melt. Further experiments are needed to verify if Pu(VI) yields higher solubility as compared to Pu(III). In case of an analogy of Pu(VI) and U(VI) behavior in borosilicate glasses, a solubility limit around 40 wt% would be expected. This might open new possibilities to increase Pu solubility in vitrification processes.

References

[1] Rothe, J. et al., *Rev. Sci. Instrum.*, **83**: 043105 (2012).

[2] Zimina, A. et al., *J. Phys.: Conf. Series*, **712**: 012019 (2016).

[3] Deschanels, X. et al., *Prog. Nucl. Ener.*, **49**: 623 (2007).

[4] Vitova, T. et al., *Inorg. Chem.*, **54**: 174 (2008).

[5] Pidchenko, I. et al., *Environ. Sci. & Technol.*, **51**: 2217 (2017).

[6] Vitova, T. et al., in print, *Nature Comm.* (2017).